Pramana – J. Phys. (2018) 91:25
https://doi.org/10.1007/s12043-018-1600-7

Meyer–Neldel energy in Se-based binary and ternary chalcogenide glasses

RAM MURTI*, S K TRIPATHI, NAVDEEP GOYAL and SATYA PRAKASH

Centre of Advanced Study in Physics, Department of Physics, Panjab University, Chandigarh 160 014, India
*Corresponding author. E-mail: rammurtisharma07@gmail.com

MS received 9 June 2017; revised 29 December 2017; accepted 29 January 2018; published online 11 July 2018

Abstract. The integral equations for DC conductivity and external conductance for the network of localised states in amorphous solids are solved by iteration method. The random free energy barriers and single polaron hopping model are used to obtain the DC conductivity σ_{DC} and Meyer–Neldel energy E_{MN}. The experimental estimates of optical band gap E_g, dielectric function ϵ, glass transition temperature T_g and σ_{DC} are used to calculate E_{MN} for Se-based binary and ternary chalcogenide glasses. The calculated values are found to be in agreement with the available experimental data. E_{MN} increases with increase of attempt frequency. The true pre-exponential factor σ_{00} is related to E_{MN} as $\ln \sigma_{00} = p - qE_{MN}$, where p is nearly 7.3 and q is material-dependent. The calculated values of E_{MN} and σ_{00} suggest that DC conduction in these chalcogenides is due to acoustic and optical phonon-assisted polaron hopping.

Keywords. Chalcogenide glasses; Meyer–Neldel energy; DC conductivity; defect density; polaron hopping; band gap.

PACS Nos 71.55.Gs; 72.80.Ey

1. Introduction

The general expression for DC conductivity, σ_{DC}, is [1]

$$\sigma_{DC} = \sigma_0 \exp\left(\frac{-E_{DC}}{k_B T}\right), \quad (1)$$

where σ_0 is the pre-factor, E_{DC} is the barrier height for DC conduction at temperature T and k_B is the Boltzmann constant. The Meyer–Neldel (MN) rule is an empirical relation between σ_0 and E_{DC} and it is stated as

$$\sigma_0 = \sigma_{00} \exp\left(\frac{E_{DC}}{E_{MN}}\right), \quad (2)$$

where σ_{00} is the true pre-factor and $E_{MN}(= k_B T_0)$ is MN energy with material characteristic temperature T_0. The MN rule is observed in single crystals, polycrystallines, amorphous and organic solids, ionic conductors and fullerenes [2–7].

Jackson [8] found that if multitrapping transport process over fixed distance is temperature-dependent, MN rule should be observed. Other researchers attribute the MN rule to the effect of disorder within the material [9–11]. Shimakawa and Abdel-Wahab [12] fitted the experimental data of DC conductivity of chalcogenide glasses As–Se–S, As–Se–I and Se–S–Te in log scale of eq. (2) and obtained the set of values of σ_{00} and E_{MN} within the range of 10^{-5} to 10^{-15} S cm^{-1} and 25 to 60 meV respectively. Small values of σ_{00} suggest that DC transport is due to tunnelling of holes through interlayer potential barriers as most of these chalcogenide glasses have two-dimensional layered structure. Yelon and Movaghar [13,14] used multimode boson field to evaluate two-level hopping rate and found that MN rule exists even for large activation energies.

It is believed that DC conductivity in chalcogenide glasses at relatively higher temperature is dominated by free holes in the valence band. Therefore, standard band transport model is not applicable to chalcogenide glasses [15]. Emin *et al* [16] proposed small polaron hopping mechanism for DC conduction in chalcogenide glasses and suggested that MN rule is the consequence of carrier-induced softening of phonon modes. In this model, σ_{00} is predicted to be of the order of 10^2 to 10^3 S cm^{-1}. The conventional correlated barrier

hopping (CBH) model [17] for σ_{DC} for chalcogenide glasses is also augmented to obtain MN rule [18–20].

Here we use the extended pair model and random free energy barriers for the network of localised states in the chalcogenide glasses to calculate σ_{DC} and E_{MN} [21,22]. It is found that E_{MN} originates from temperature-induced configurational and electronic entropies. The parameters used in the calculations are adopted from the estimates of available experimental data in the literature. The calculated values of E_{MN} for binary and ternary chalcogenide glasses $Se_{1-x}X_x$ (X = Ge, In, Te) and $Se_{1-x-y}Te_xX_y$ (X = Ge, In) are found to be in agreement with the experimental data and other theoretical results. The correlations between E_{MN} and jump frequency and between $\ln \sigma_{00}$ and E_{MN} are also studied.

The plan of the paper is as follows: The necessary formalism is presented in §2 and the results are discussed in §3.

2. Formalism

Summerfield and Butcher [23,24] solved Kirchhoff's equations for a network of localised states in amorphous solids in the extended pair model using two site approximations. The resulting integral equation for DC hopping conductivity is obtained as

$$\sigma_{DC} = \frac{4\pi N_s^2}{6} \int_{r_{min}}^{r_{max}} dr\, r^4 \left[\frac{1}{g(E,r)} + \frac{2}{Y(E)}\right]^{-1}, \quad (3)$$

where N_s is the density of defect sites and r_{min} and r_{max} are the minimum and maximum defect site separations. The internal conductance $g(E,r)$ between the defect sites of energy E at the separation r is given as

$$g(E,r) = g_0 \exp\left(\frac{-E_{DC}}{k_B T}\right) \quad (4)$$

and the external conductance $Y(E)$ is

$$Y(E) = \frac{4\pi N_s}{B_P} \int_{r_{min}}^{r_{max}} dr\, r^2 \left[\frac{1}{g(E,r)} + \frac{1}{Y(E)}\right]^{-1}, \quad (5)$$

where g_0 and $(1/B_p)$ are the proportionality constants. If we use the limits $(Y(E)/g(E,r)) \simeq 0$ and $r_{min} \simeq 0$ in eq. (5), we get $r_{max} = r_p$, which is the percolation radius and it is given as

$$r_p = \left(\frac{3B_p}{4\pi N_s}\right)^{1/3}. \quad (6)$$

Here $(1/B_p)$ is determined with the predictions of percolation theory and for three-dimensional solids, $B_p = 2.7$ [25].

Further, eq. (5) is solved by iterative method. In the first iteration, it is assumed that external and internal conductances are equal at r_p, i.e.

$$Y(E) = g(E,r_p) = g_0 \exp\left(\frac{-E_{DC}(r_p)}{k_B T}\right). \quad (7)$$

There is temperature-induced configurational and electronic disorder in the thermally activated DC conduction in the amorphous solids. Therefore, E_{DC} will involve thermal fluctuations and hence a range of activation energies will contribute to the conduction process. Thus, E_{DC} will represent a distribution of free energy barriers and for the random free energy barrier distribution

$$E_{DC}(r,T) = E^0_{DC}(r) - TS, \quad (8)$$

where $E^0_{DC}(r)$ is the temperature-independent barrier height and S is the entropy. Here, $E^0_{DC}(r)$ is compensated by thermal fluctuations TS. In the CBH model [17]

$$E^0_{DC}(r) = E_M - \frac{4ze^2}{\epsilon r}, \quad (9)$$

where E_M is the maximum barrier height, ϵ is the dielectric constant and $z = 1$ and 2 for single and bipolaron hopping conduction respectively.

Use of eqs (7)–(9) in eq. (5) gives

$$Y(E) = \frac{4\pi N_s}{B_p} g(E,r_p) \times \int_{r_{min}}^{r_{max}} dr\, r^2 \left[\frac{1}{1 + g(E,r_p)/g(E,r)}\right], \quad (10)$$

where

$$g(E,r_p)/g(E,r) = \exp\left[a\left(\frac{1}{r_p} - \frac{1}{r}\right)\right] \quad (11)$$

and

$$a = \frac{4ze^2}{\epsilon k_B T}. \quad (12)$$

For further simplification of eq. (10), it is assumed that $r_{max} \simeq r_p$, $g(E,r_p)/g(E,r) \ll 1$ and $r_p^3 \gg r_{min}^3$ [21, 24]. This gives

$$Y(E) \simeq \frac{4\pi N_s}{3B_p} g(E,r_p) r_p^3 \quad (13)$$

and

$$Y(E)/g(E,r) = \frac{4\pi N_s}{3B_p} r_p^3 \frac{g(E,r_p)}{g(E,r)}. \quad (14)$$

Using similar simplifications in eq. (3) and assuming that $r_p^5 \gg r_{min}^5$, one gets

$$\sigma_{DC} = \frac{4\pi N_s^2}{6} \frac{Y(E)}{10} r_p^5. \quad (15)$$

The use of eqs (7) and (13) simplifies eq. (15) as

$$\sigma_{\mathrm{DC}} = \frac{\pi N_s^2 r_p^5}{15} g(E, r_p). \tag{16}$$

Further use of eqs (7) and (8) in eq. (16) gives

$$\sigma_{\mathrm{DC}} = \frac{\pi N_s^2 r_p^5}{15} g_0 \exp\left(\frac{S}{k_{\mathrm{B}}}\right) \exp\left(\frac{-E_{\mathrm{DC}}^0(r_p)}{k_{\mathrm{B}} T}\right). \tag{17}$$

Thus, the MN rule in σ_{DC} is achieved due to entropy of the material.

Using dimensional considerations in eq. (17), we write [24]

$$g_0 \exp\left(\frac{S}{k_{\mathrm{B}}}\right) = C\omega_0 \exp\left(\frac{E_{\mathrm{DC}}^0(r_p)}{E_{\mathrm{MN}}}\right), \tag{18}$$

where C and ω_0 have the dimensions of capacitance and frequency respectively and

$$E_{\mathrm{MN}} = \frac{k_{\mathrm{B}} E_{\mathrm{DC}}^0(r_p)}{S} = k_{\mathrm{B}} T_0. \tag{19}$$

Here, T_0 is the characteristic temperature of the material as discussed earlier. Evidently, E_{MN} will increase with increase of E_{DC}^0 and will decrease with increase of S. However, for a given E_{DC}^0, E_{MN} may not be observable for large values of S.

As both C and ω_0 increase with increase of temperature, it is difficult to establish the exact temperature dependence of $C\omega_0$ [26]. Therefore, $C\omega_0$ is taken as temperature-independent and it is written in conventional units as [27]

$$C\omega_0 = \alpha\left(\frac{e^2}{\pi k_{\mathrm{B}} \theta_{\mathrm{D}}}\right) \nu_0, \tag{20}$$

where θ_{D} and ν_0 are Debye temperature and effective jump frequency respectively and α is the magnitude parameter of $C\omega_0$. These parameters essentially represent the material properties.

The use of eqs (18)–(20) in eq. (17) gives

$$\sigma_{\mathrm{DC}} = \sigma_{00} \exp\left(\frac{E_{\mathrm{DC}}^0}{E_{\mathrm{MN}}}\right) \exp\left(-\frac{E_{\mathrm{DC}}^0}{k_{\mathrm{B}} T}\right), \tag{21}$$

where the pre-factor

$$\sigma_0 = \sigma_{00} \exp\left(\frac{E_{\mathrm{DC}}^0}{E_{\mathrm{MN}}}\right) \tag{22}$$

and true pre-factor

$$\sigma_{00} = \alpha\left(\frac{e^2 N_s^2 r_p^5}{15 k_{\mathrm{B}} \theta_{\mathrm{D}}}\right) \nu_0. \tag{23}$$

Here, DC conduction is due to phonon-assisted single polaron hopping. As temperature decreases, S will decrease and E_{MN} will increase. Consequently, σ_{DC} will decrease. Similarly, σ_{DC} will increase with increase of T. Thus, entropy barrier height TS is significant in the DC conduction process and MN rule arises due to temperature-induced configurational and electronic entropies.

For further discussion, we rewrite eq. (23) with the help of eq. (6) as

$$\sigma_{00} = \frac{\alpha e^2 \nu_0}{15 k_{\mathrm{B}} \theta_{\mathrm{D}}} \left(\frac{3B_p}{4\pi}\right)^{5/3} N_s^{1/3}. \tag{24}$$

Thus, σ_{00} explicitly depends on attempt frequency ν_0 and defect density N_s. As the chalcogenide melt is quenched at glass transition temperature T_{g}, N_s is given as [28]

$$N_s = N_0 \exp(-E_{\mathrm{VAP}}/2k_{\mathrm{B}} T_{\mathrm{g}}), \tag{25}$$

where the concentration of chalcogen atoms

$$N_0 \approx 2\left(\frac{2\pi m_w k_{\mathrm{B}} T_{\mathrm{g}}}{h^2}\right)^{3/2} \tag{26}$$

and m_w is the effective atomic mass of the chalcogen atom. The factor 2 is added, as the defect states are doubly occupied. E_{VAP} is the energy needed to create a valence alternation pair and $E_{\mathrm{VAP}}/2$ is nearly the Fermi energy position. Therefore, we assume that $E_{\mathrm{VAP}} \approx E_{\mathrm{DC}}$, the estimated barrier height from the experimental data of σ_{DC} [29,30].

We can also write eq. (24) with the help of eqs (25) and (26) as

$$\ln \sigma_{00} = p - q E_{\mathrm{MN}}, \tag{27}$$

where

$$p = \ln \alpha + (1/3)\ln 2 + (5/3)\ln(3B_p/4\pi) + \ln(e^2 \nu_0/15 k_{\mathrm{B}} \theta_{\mathrm{D}}) + (1/2)\ln(2\pi m_w k_{\mathrm{B}} T_{\mathrm{g}}/h^2) \tag{28}$$

$$q = \frac{xy}{3k_B T_g}, \quad x = (E_{\mathrm{DC}}/E_{\mathrm{DC}}^0) \quad \text{and} \quad y = (S/k_{\mathrm{B}}). \tag{29}$$

Thus, $\ln \sigma_{00}$ is linearly related to E_{MN}, and the intercept p and slope q will depend on material properties and the experimental conditions.

3. Results and discussion

We rewrite eq. (21) as

$$E_{\mathrm{MN}} = \frac{E_{\mathrm{DC}}^0}{\left[\left(\frac{E_{\mathrm{DC}}^0}{k_{\mathrm{B}} T} + \ln\left(\frac{\sigma_{\mathrm{DC}}}{\sigma_{00}}\right)\right)\right]}. \tag{30}$$

The parameters E^0_{DC}, T, σ_{DC}, N_s, θ_D and ν_0 are needed to calculate E_{MN}. σ_{DC} and T are the experimental data. E^0_{DC} is calculated by replacing r by r_p in eq. (9) and using the relation $E_M = 2(E_g - E^0_{DC})$, where E_g is the optical band gap. This gives

$$E^0_{DC} = (1/3)\left(2E_g - \frac{4ze^2}{\epsilon r_p}\right). \tag{31}$$

r_p and N_s are calculated with the help of eqs (6) and (25) respectively. The glass transition temperature T_g varies with heating rate β, and therefore T_g is estimated with the empirical relation

$$T_g = A + B\log(\beta), \tag{32}$$

where the parameters A and B are the intercepts and slopes of T_g vs. $\log\beta$ graph [31].

θ_D for Se-based binary and ternary chalcogenide glasses is estimated with the help of Debye temperature θ'_D of amorphous Ge, Se, Te and In. Here, $\theta'_D = 244.6$ K for a-Ge is taken from the calculations of Singh and Ali [32] and $\theta'_D = 67$ K for a-In is taken from Comberg *et al* [33]. The specific heat measurements of amorphous and crystalline Se predict $\theta'_D = 56$ K and 90 K respectively [34,35]. θ'_D for a-Te is not available, and therefore we estimated $\theta'_D = 95$ K for a-Te by reducing its crystalline value $\theta'_D = 153$ K in the same ratio as for a-Se given above. The weighted average of these values of θ'_D is taken as θ_D for these alloys. If $\nu_0 = \nu_D$, where ν_D is the Debye frequency, it is calculated as $h\nu_D = k_B\theta_D$. The details of other parameters are as follows:

(a) $Se_{100-x}Ge_x$ ($x = 15, 20, 25$)

Zolanvari *et al* [36] prepared glassy alloys $Se_{100-x}Ge_x$ ($x = 15, 20, 25$) by heating and quenching (HQ) rate and measured the DC conductivity σ_{DC}. We adopted σ_{DC}, T and E_{DC} from these measurements. N_s is estimated with the help of eq. (25) and m_w is taken as the weighted average atomic mass of $Se_{100-x}Ge_x$ alloy.

Craig Russel [37] studied the photodarkening properties of Ge–Se glasses using both the curve fitting and derivative techniques to obtain E_g and ϵ. These results were close to those obtained by Shirafuji *et al* [38] with the help of photoluminisence and absorption spectra of $Se_{1-x}Ge_x$ compounds and those obtained by Oheda [39] with the help of compositional dependence of Urbash tail of these glasses. Sharma and Kumar [40] estimated ϵ from the capacitance measurements of the thin films. Therefore, we have taken E_g and ϵ from the estimates of Craig Russel [37].

Derrey *et al* [41] prepared the amorphous $Se_{85}Ge_{15}$ by HQ method and estimated $T_g = 408$ K with the help of structural relaxation data obtained by differential thermal analysis (DTA). Tiwari *et al* [42] also prepared $Se_{80}Ge_{20}$ alloy by the same method. However, they analysed the differential scanning calorimetric (DSC) data for different heating rates. We calculated T_g with the help of eq. (32) using parameters $A = 378.1$, $B = 17.1$ and the average value of $\log\beta = 3.0$ given by them. Hyun-Yong *et al* [43] analysed DTA data of $Se_{75}Ge_{25}$ and estimated $T_g = 493$ K.

(b) $Se_{100-x}In_x$ ($x = 10, 15, 20$)

Mehta *et al* [44] measured DC and AC conductivities of $Se_{100-x}In_x$ ($x = 10, 15, 20$) glassy alloys prepared by HQ technique and estimated E_{DC}. They also estimated ϵ and T_g with the help of capacitance and AC conductivity measurements respectively. We have taken σ_{DC}, T, E_{DC}, ϵ and T_g from them. Singh *et al* [45] also prepared $Se_{100-x}In_x$ glasses by HQ method and estimated E_g by analysing the reflection spectra and found a non-linear relation between E_g and x. We have adopted these values of E_g for our calculations [45]. N_s and m_w are estimated as for $Se_{100-x}Ge_x$ alloys.

(c) $Se_{100-x}Te_x$ ($x = 10, 20, 30$)

Mehra *et al* [46] used HQ method to prepare $Se_{100-x}Te_x$ ($x = 10, 20, 30$) glasses and measured σ_{DC} in the temperature range 150 K to 300 K. We have taken σ_{DC}, E_{DC} and T from these measurements. N_s and m_w are calculated as for $Se_{100-x}Ge_x$ alloys.

Calventus *et al* [47] prepared the glassy alloys $Se_{90}Te_{10}$ by HQ method and obtained $T_g = 320$ K by analysing the X-ray diffraction data with the help of crystallisation rate equation. Mehta *et al* [48] analysed the DSC thermograms of glassy $Se_{80}Te_{20}$ and estimated the parameters A, B and β. We obtained $T_g = 342$ K with the help of eq. (32) with $A = 328.7$, $B = 11.83$ and average value of $\log\beta = 1.2$ given by Mehta *et al* [48]. Similarly, the DSC thermogram analysis of $Se_{70}Te_{30}$ glasses due to Srivastava *et al* [49] gave $T_g = 357$ K with $A = 338.88$, $B = 6.80$ and average value of $\log\beta = 2.7$.

E_g and ϵ for the configuration $Se_{100-x}Te_x$ ($x = 10, 15, 20$) is not available to us. Therefore, we estimated these parameters with the help of linear relation between E_g and ϵ given by Mandoza-Galvan *et al* [50] from their measurements of transmission and reflectivity of amorphous Se_xTe_{1-x} alloys.

(d) $Se_{85-x}Te_{15}Ge_x$ ($x = 2, 6, 10, 15$)

Kumar *et al* [51] prepared $Se_{85-x}Te_{15}Ge_x$ ($x = 2, 6, 10, 15$) alloys by HQ method and measured σ_{DC} in the temperature range of 279–353 K. We have taken σ_{DC}, T and E_{DC} from these measurements. Kumar *et al* [52] also reported the temperature and frequency dependence

of ϵ of these alloys in the frequency range 5 kHz to 20 kHz and in the temperature range 253–313 K. There is dispersion in ϵ with frequency, and therefore we have taken ϵ at the highest frequency 20 kHz and at $T = 303$ K. N_s and m_w are estimated as for $Se_{100-x}Ge_x$ glasses.

T_g is not available for $Se_{85-x}Te_{15}Ge_x$ alloys. Patial *et al* [53] prepared $Se_{85-x}Te_{15}Sn_x$ ($x = 0, 2, 4$ and 6) glasses by HQ method and estimated T_g with the help of DSC data and crystallisation rate equation. Similar measurements are also carried out for $Se_{85-x}Te_{15}Bi_x$ glasses [54]. As the atomic mass of Ge is closer to Sn, we estimated T_g for $Se_{85-x}Te_{15}Ge_x$ ($x = 2, 6, 10, 15$) alloys from the linear relation of T_g and x for $Se_{85-x}Te_{15}Sn_x$ [53]. Ganesan *et al* [55] prepared $Se_{100-x-y}Te_yGe_x$ glasses using HQ technique and used photoacoustic data to estimate the dependence of E_g on average coordination number Z_a given as

$$Z_a = \frac{xZ_{Ge} + yZ_{Te} + (100 - x - y)Z_{Se}}{100}, \tag{33}$$

where $Z_{Ge} = 4$, $Z_{Te} = 2$ and $Z_{Se} = 2$ are the coordination numbers of Ge, Te and Se respectively. We calculated Z_a for the configurations $Se_{85-x}Te_{15}Ge_x$ ($x = 2, 6, 10, 15$) using eq. (33) and estimated E_g with the illustration given by Ganesan *et al* [55] for the lowest Te concentration $Ge_xSe_{80-x}Te_{20}$ alloy.

(e) $Se_{85-x}Te_{15}In_x$ ($x = 2, 6, 10, 15$)

Kumar *et al* [56,57] also measured and estimated σ_{DC}, T, E_{DC} and ϵ for $Se_{85-x}Te_{15}In_x$ ($x = 2, 6, 10, 15$) alloys as discussed for $Se_{85-x}Te_{15}Ge_x$ alloys. We have taken these parameters from the above measurements and estimates. N_s and m_w are calculated as described earlier.

Tripathi *et al* [58] did the DSC measurements for $Se_{70}Te_{15}In_{15}$ alloy at different heating rates and used crystallisation rate equation to obtain T_g. We have taken $T_g = 349$ K, and the average of T_g given for different heating rates. Similar measurements of Patial *et al* [59] suggested $T_g = 340$ K for the $Se_{79}Te_{15}In_6$ configuration. T_g for the configurations $Se_{83}Te_{15}In_2$ and $Se_{75}Te_{15}In_{10}$ is not available. Therefore, we linearly extrapolated the data of [58,59] to obtain T_g for these configurations.

The increase of σ_{DC} is not linear with increase of In concentration in $Se_{85-x}Te_{15}In_x$ alloys. σ_{DC} is maximum for $x = 10$. As discussed earlier, Singh *et al* [45] found non-linear relation between E_g and x for $Se_{100-x}In_x$ alloys and E_g is minimum for $x = 10$. The In impurity-induced crystallisation will reduce the band gap. Therefore, we estimated E_g for $Se_{100-x}Te_{15}In_x$ alloys using the graphical relation given in [45] assuming that E_g will be less than those for $Se_{100-x}Te_x$ alloys.

The input parameters E_g, ϵ, m_w, T_g, θ_D, E_{DC}, T and σ_{DC} are tabulated in table 1 for binary and ternary alloys respectively. These parameters are used to calculate σ_0, σ_{00} and E_{MN} with the help of eqs (22), (23) and (30) respectively for $\alpha = 1$. These results along with N_s, r_p, ν_D, E^0_{DC}, p and q are tabulated in table 2.

It is noted that σ_{DC} for $Se_{100-x}Ge_x$ alloys is larger by three to four orders of magnitude than those for $Se_{100-x}In_x$ alloys and six to seven orders of magnitude larger than those of $Se_{100-x}Te_x$ alloys. The addition of Ge in $Se_{100-x}Te_x$ alloys does not alter σ_{DC} significantly while with addition of In in $Se_{100-x}Te_x$ alloys, σ_{DC} increases nearly by four to five orders of magnitude. Further in the formation of ternary alloy, the Ge impurity in $Se_{100-x}Te_x$ reduces N_s nearly by four orders, while In impurity increases N_s by four to six orders. N_s is minimum and maximum for $Se_{85-x}Te_{15}Ge_x$ and $Se_{85-x}Te_{15}In_x$ alloys respectively and this is consistent with the variation of σ_{DC}. The percolation radius r_p is sufficiently large for $Se_{100-x}Te_x$ and $Se_{85-x}Te_{15}Ge_x$ alloys and it is nearly of the order of nearest neighbour distances for $Se_{85-x}Te_{15}In_x$ alloys.

In $Se_{100-x}In_x$ and $Se_{85-x}Te_{15}In_x$ alloys, E^0_{DC} is nearly twice of E_{DC}, in $Se_{100-x}Ge_x$ and $Se_{100-x}Te_x$ alloys E^0_{DC} is nearly 50% higher than E_{DC} and in $Se_{85-x}Te_{15}Ge_x$ alloys, E^0_{DC} is about 15% higher than E_{DC}. Thus, thermal compensation is the significant part of DC conduction barrier height.

E_{MN} increases from 67 to 75 meV with increase in Te concentration in $Se_{100-x}Te_x$ alloys while it remains nearly 40 meV with increase of Ge concentration in $Se_{100-x}Ge_x$ alloys. In $Se_{100-x}In_x$ alloys, E_{MN} increases from 47 to 72 meV with the minimum for $x = 15$. E_{MN} increases from 52 to 59 meV with increase of Ge concentration in $Se_{85-x}Te_{15}Ge_x$ alloys while in $Se_{85-x}Te_{15}In_x$ alloys, E_{MN} is varying inconsistently within 57 to 51 meV with an exception of 97 meV for $x = 10$. The magnitude of our calculated values of E_{MN} agrees with the estimates of Shimakawa and Abdel-Wahab [12] for the As-based chalcogenides.

(f) Correlations between E_{MN}, ν_0, σ_{00}, σ_0 and E^0_{DC}

It was shown by Miller and Abrahams [60] that effective jump frequency at higher temperature is given as $\nu_0 \approx 2 \times 10^{12}(r/R)^{3/2} \exp(-2r/R)$ where (r/R) is the ratio of intersite separation r and radius of localised polaron states R. Therefore, we studied the variation of E_{MN} with ν_0 in the the frequency range (10–100) $\times 10^{12}$ Hz for both binary and ternary alloys. These results are shown in figures 1a–1e. In the above frequency range, E_{MN} increases within 10% for $Se_{100-x}Ge_x$ alloys while for $Se_{100-x}Te_x$ alloy, E_{MN} increases by about 30% for all the values of x. This increase in E_{MN} in the above frequency range is 40% for $x = 20$, 16% for $x = 10$

Table 1. Physical parameters of binary chalcogenides $Se_{100-x}Ge_x$, $Se_{100-x}In_x$ and $Se_{100-x}Te_x$ (A) and ternary chalcogenides $Se_{85-x}Te_{15}Ge_x$ and $Se_{85-x}Te_{15}In_x$ (B).

Chalcogenide	E_g (eV)	ϵ	m_w (a.m.u.)	T_g (K)	θ_D (K)	E_{DC} (eV)	T (K)	σ_{DC} (Ω^{-1} cm^{-1})
(A)								
$Se_{85}Ge_{15}$	1.97	5.9	78.01	408	84.29	0.93	333	$1.08E-5$
$Se_{80}Ge_{20}$	2.00	5.7	77.69	430	93.70	0.76	333	$8.98E-6$
$Se_{75}Ge_{25}$	2.06	5.5	77.38	493	103.15	0.90	333	$9.77E-6$
$Se_{90}In_{10}$	2.00	3.0	82.55	335	57.10	0.51	307	$2.33E-9$
$Se_{85}In_{15}$	2.23	3.0	84.34	338	57.65	0.63	307	$9.87E-11$
$Se_{80}In_{20}$	2.21	3.0	86.13	337	58.20	0.41	307	$3.34E-7$
$Se_{90}Te_{10}$	1.69	7.0	83.82	320	59.90	0.77	300	$6.13E-13$
$Se_{80}Te_{20}$	1.54	7.5	88.69	342	63.80	0.72	300	$6.04E-12$
$Se_{70}Te_{30}$	1.46	8.5	93.55	357	67.70	0.68	300	$6.00E-11$
(B)								
$Se_{83}Te_{15}Ge_2$	1.78	10.2	86.13	338	65.62	1.05	303	$2.40E-12$
$Se_{79}Te_{15}Ge_6$	1.72	7.90	85.87	340	73.17	1.06	303	$2.06E-12$
$Se_{75}Te_{15}Ge_{10}$	1.70	6.00	85.62	345	80.71	1.04	303	$2.26E-12$
$Se_{70}Te_{15}Ge_{15}$	1.65	4.50	85.31	350	90.14	0.99	303	$2.79E-12$
$Se_{83}Te_{15}In_2$	1.46	19.6	86.97	337	62.07	0.43	293	$8.56E-8$
$Se_{79}Te_{15}In_6$	1.40	24.9	88.41	340	62.51	0.49	293	$7.19E-8$
$Se_{75}Te_{15}In_{10}$	1.25	43.2	89.84	344	62.95	0.29	293	$1.70E-6$
$Se_{70}Te_{15}In_{15}$	1.48	70.0	91.63	349	63.50	0.44	293	$1.32E-7$

E_g (eV): Estimated band gap from optical transmission measurements, ϵ: Estimated dielectric constant from optical transmission and capacitance measurements, m_w (a.m.u.): Weighted average atomic mass of the chalcogenide, T_g: Estimated glass transition temperature from calorimetric measurements, θ_D (K): Weighted averaged Debye temperature estimated from Debye temperature of amorphous constituent elements, E_{DC} (eV): Experimental DC activation energy, σ_{DC} (Ω^{-1} cm^{-1}): Experimental DC conductivity at temperature T (K).

and 10% for $x = 15$ in the $Se_{100-x}In_x$ alloys. Similarly, E_{MN} increases about 15% for given concentrations of Ge in the $Se_{85-x}Te_{15}Ge_x$ alloys. However, this increase of E_{MN} is 10% for $x = 2, 6, 15$ and 100% for $x = 10$ in the $Se_{85-x}Te_{15}In_x$ alloys. Thus, the increase in E_{MN} with increase of ν_0 depends upon both impurity concentration and its characteristics.

The correlations between $\ln \sigma_{00}$ and E_{MN}, as given in eq. (27), for these alloys are shown in figures 2a–2e. The results tabulated in table 2 show that, p is nearly 7.3 for all these alloys and this agrees with the results obtained by Yelon and Movaghar [14]. However, q depends on the material properties. It is larger for alloys with Ge impurities than those alloys with Te and In impurities. The best-fit linear relations $\ln \sigma_{00} = p_1 - q_1 E_{MN}$ through these points with constants p_1 and q_1 are shown by solid lines in figures 2a–2e. The dispersion from linearity is maximum for $Se_{85-x}Te_{15}In_x$ ternary alloys.

To obtain a unified correlation between $\ln \sigma_{00}$ and E_{MN}, $\ln \sigma_{00}$ and E_{MN} for all these alloys are put together in figure 3. The calculated results are well represented by two independent linear relations as shown by solid lines, one for $Se_{100-x}Te_x$ and $Se_{85-x}Te_{15}Ge_x$ (group A) alloys with $(p_1, q_1) = (-14.64, -0.198)$ and other for $Se_{100-x}Ge_x$, $Se_{100-x}In_x$ and $Se_{85-x}Te_{15}In_x$ (group B) alloys with $(p_1, q_1) = (-2.124, -0.078)$. However, the calculated results are too far from an overall linear relation between $\ln \sigma_{00}$ and E_{MN} with $(p_1, q_1) = (-2.95, -0.057)$ as shown by the dashed line.

The correlation between $\ln \sigma_0$ and static barrier height E^0_{DC} for these alloys is shown in figure 4. It is similar to that between $\ln \sigma_{00}$ and E_{MN}. The calculated points are too dispersed from the linear relation $\ln \sigma_0 = p_2 - q_2 E^0_{DC}$ with $(p_2, q_2) = (-9.41, -28.01)$ as shown by the dashed line. However, two linear relations for the group A and group B materials are well represented by the solid lines with $(p_2, q_2) = (-7.95, -21.64)$ and $(-7.98, -30.27)$ respectively.

E_{MN} and σ_{00} are quite sensitive to the determination of slope and intercept of $\ln \sigma_0$ vs. E_{DC} correlations. Therefore, we also studied the correlation between E_{MN} and σ_{00} with σ_{00} in the range of 10^3 to $10^{-15}\omega^{-1}$cm^{-1} as discussed in Introduction [12,16], using eq. (30). These results for the two alloys $Se_{90}Te_{10}$ and $Se_{83}Te_{15}Ge_2$ are shown in figure 5. E_{MN} varies between 135 and 22 meV for $Se_{90}Te_{10}$ alloy and between 100 and 22 meV for $Se_{83}Te_{15}Ge_2$ alloy for σ_{00} in the range of 10^3 to $10^{-15}\Omega^{-1}$cm^{-1}. E_{MN} increases with the increase of σ_{00}.

Table 2. Calculated parameters of binary chalcogenides $Se_{100-x}Ge_x$, $Se_{100-x}In_x$ and $Se_{100-x}Te_x$ (A) and ternary chalcogenides $Se_{85-x}Te_{15}Ge_x$ and $Se_{85-x}Te_{15}In_x$ (B).

Chalcogenide	N_s (cm)$^{-3}$	r_p (Å)	ν_D (10^{12} Hz)	E^0_{DC} (eV)	σ_{00} (Ω^{-1} cm^{-1})	σ_0 (Ω^{-1} cm^{-1})	E_{MN} (meV)	p (Ω^{-1} cm^{-1})	q (eV^{-1})
(A)									
$Se_{85}Ge_{15}$	$7.20E+15$	505	1.76	1.31	0.44	$6.42E+14$	37	7.38	235.25
$Se_{80}Ge_{20}$	$2.92E+18$	69	1.95	1.29	3.60	$2.52E+14$	40	7.38	169.31
$Se_{75}Ge_{25}$	$1.82E+18$	81	2.15	1.33	3.07	$1.34E+15$	39	7.46	178.63
$Se_{90}In_{10}$	$3.76E+19$	30	1.19	1.12	8.88	$5.66E+9$	55	7.30	106.47
$Se_{85}In_{15}$	$7.52E+17$	109	1.20	1.43	2.25	$2.72E+13$	47	7.32	151.87
$Se_{80}In_{20}$	$1.40E+21$	9.1	1.21	0.77	31.49	$1.46E+6$	72	7.33	65.57
$Se_{90}Te_{10}$	$1.28E+15$	894	1.25	1.12	0.24	$4.59E+6$	67	7.29	138.62
$Se_{80}Te_{20}$	$5.04E+16$	266	1.33	1.01	0.88	$7.30E+5$	74	7.35	109.04
$Se_{70}Te_{30}$	$5.94E+17$	118	1.41	0.95	2.08	$6.40E+5$	75	7.40	97.45
(B)									
$Se_{83}Te_{15}Ge_2$	$4.33E+11$	12500	1.37	1.19	0.0145	$1.30E+8$	52	7.33	231.57
$Se_{79}Te_{15}Ge_6$	$3.82E+11$	13020	1.52	1.15	0.0141	$2.41E+7$	54	7.33	223.30
$Se_{75}Te_{15}Ge_{10}$	$1.29E+12$	8732	1.68	1.13	0.0216	$1.57E+7$	56	7.34	209.73
$Se_{70}Te_{15}Ge_{15}$	$1.13E+13$	4266	1.88	1.09	0.0460	$5.30E+6$	59	7.34	184.48
$Se_{83}Te_{15}In_2$	$7.14E+20$	11	1.29	0.89	24.83	$1.55E+8$	57	7.33	86.93
$Se_{79}Te_{15}In_6$	$1.09E+20$	21	1.30	0.89	12.88	$1.91E+8$	54	7.35	102.50
$Se_{75}Te_{15}In_{10}$	$1.17E+23$	2.1	1.31	0.62	148.01	$8.85E+4$	97	7.36	33.41
$Se_{70}Te_{15}In_{15}$	$9.70E+20$	10	1.32	0.96	27.65	$4.28E+9$	51	7.38	95.66

N_s (cm^{-3}): Defect density, r_p (Å): Percolation radius, ν_D (10^{12} Hz): Debye frequency, E^0_{DC} (eV): DC conduction static barrier height, σ_{00} (Ω^{-1}cm^{-1}): True prefactor, σ_0 (Ω^{-1} cm^{-1}): Prefactor, E_{MN} (meV): Meyer–Neldel energy, p (Ω^{-1} cm^{-1}) and q (eV^{-1}): Parameters as discussed in the text.

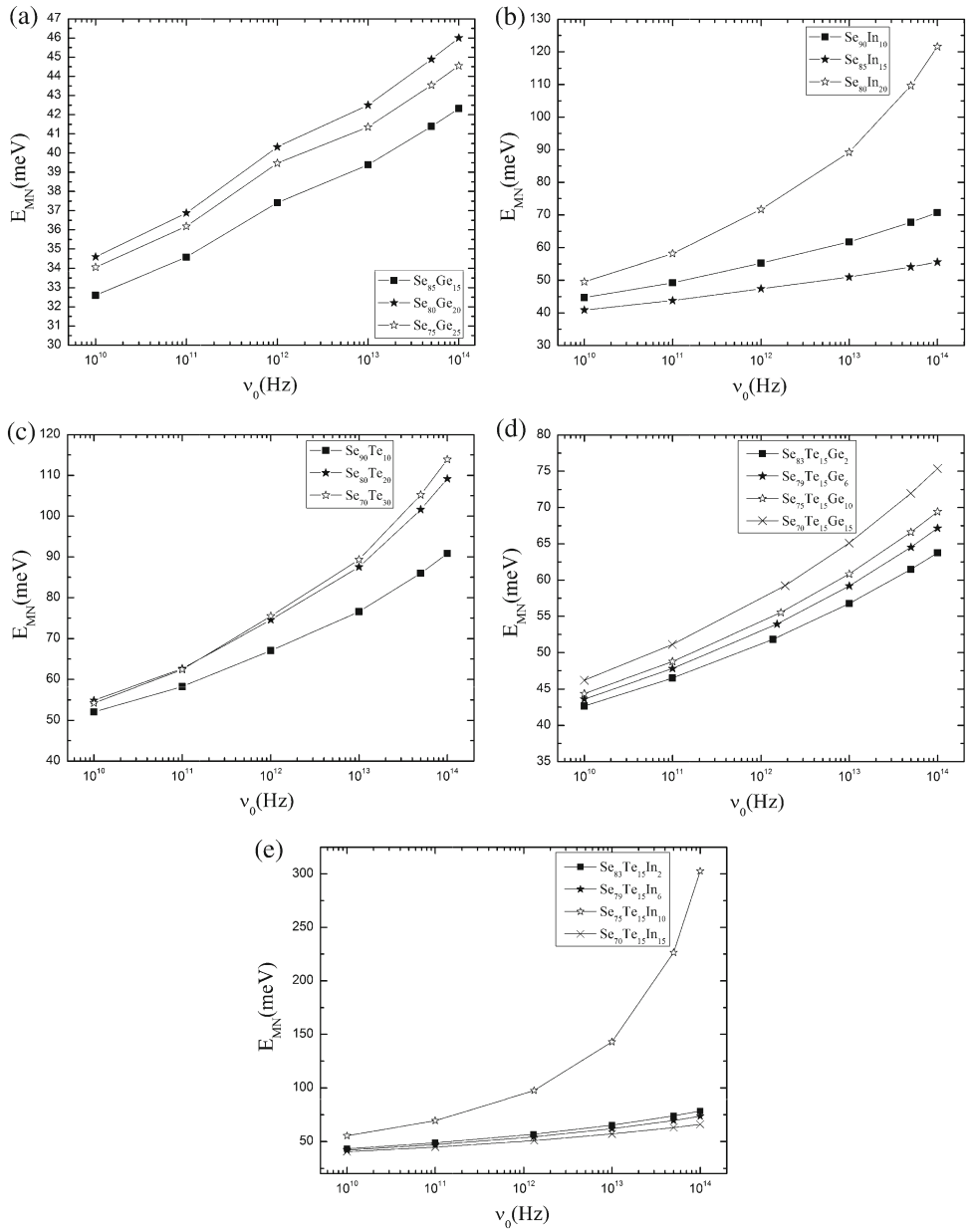

Figure 1. The variation of E_{MN} with frequency ν_0 for **(a)** $Se_{100-x}Ge_x$, **(b)** $Se_{100-x}In_x$, **(c)** $Se_{100-x}Te_x$, **(d)** $Se_{85-x}Te_{15}Ge_x$ and **(e)** $Se_{85-x}Te_{15}In_x$.

(g) Comparison of E_{MN} with experiments

It is interesting to study the correlation between the calculated and available experimental values of E_{MN}. Mehta *et al* [61] prepared the $Se_{100-x}Ge_x$ ($5 \leq x \leq 22$), $Se_{100-x}In_x$ ($5 \leq x \leq 30$) and $Se_{100-x}Te_x$ ($5 \leq x \leq 30$) alloys by HQ method and studied the DSC pattern at the cooling rate of 5 K/min. These results are used in the crystallisation rate equation (CRE) to estimate E_{MN}. These values are 39, 36 and 32 meV for $Se_{100-x}Ge_x$, $Se_{100-x}In_x$ and $Se_{100-x}Te_x$ alloys respectively. Muiva *et al* [62] also prepared the glassy alloy $Se_{100-x}In_x$ ($1 \leq x \leq 20$) by the same method and used the DSC data in CRE and estimated $E_{MN} = 48$ meV for $Se_{100-x}In_x$ alloys.

We have calculated E_{MN} for these alloys using DC conduction rate equation and the calculated values of E_{MN} for $Se_{100-x}Ge_x$ ($15 \leq x \leq 25$) alloys are between 30 and 40 meV. If it is assumed that E_{MN} obtained through CRE is the impurity averaged concentration value of E_{MN}, our results for $Se_{100-x}Ge_x$ alloy agree with those obtained by Mehta and Kumar [61]. Our calculated values of E_{MN} for $Se_{100-x}In_x$ ($10 \leq x \leq 20$) alloys are between 47 and 72 meV. These values are higher than those estimated by Mehta and Kumar [61]. However, the values agree with those of Muiva *et al* [62].

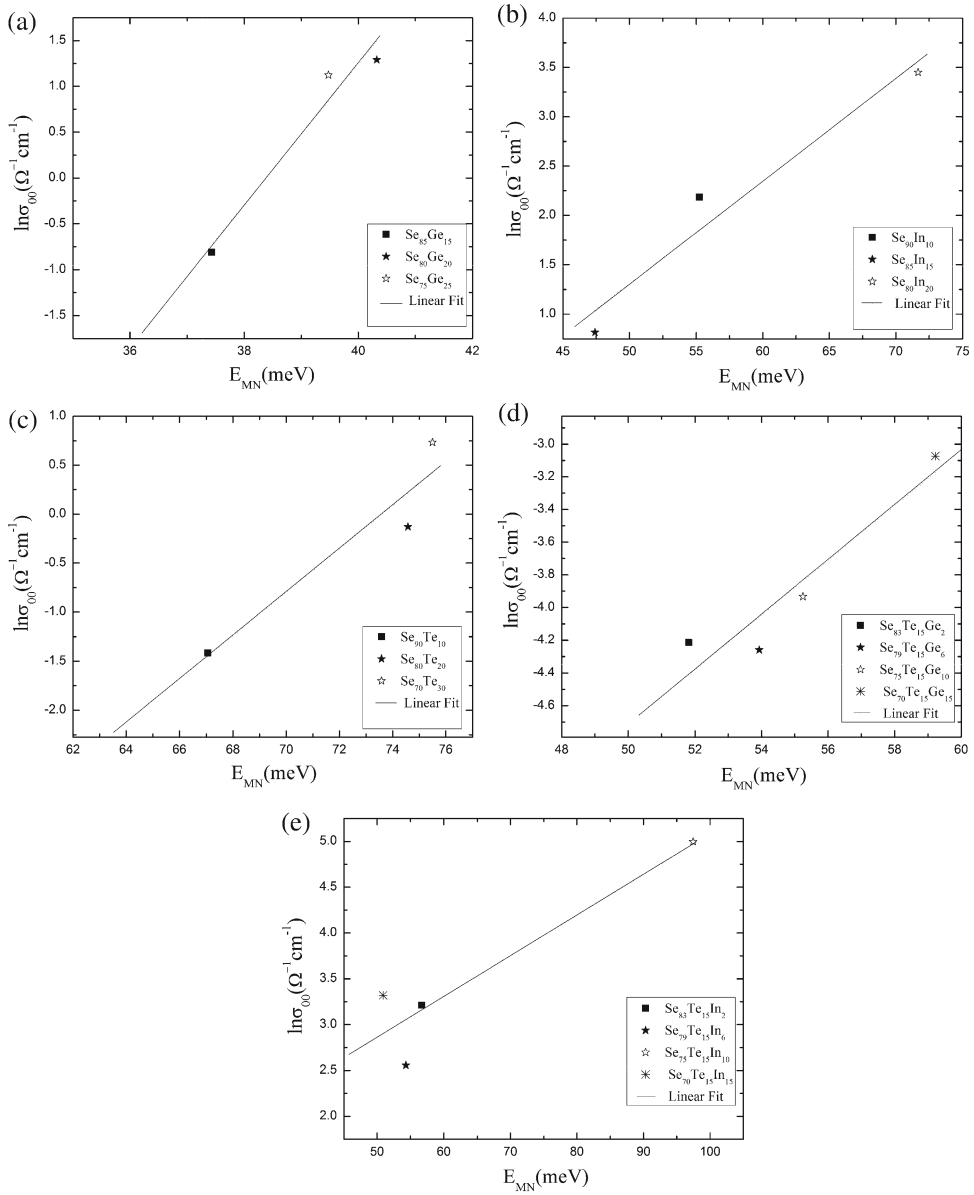

Figure 2. $\ln\sigma_{00}$ vs. E_{MN} for **(a)** $Se_{100-x}Ge_x$, **(b)** $Se_{100-x}In_x$, **(c)** $Se_{100-x}Te_x$, **(d)** $Se_{85-x}Te_{15}Ge_x$ and **(e)** $Se_{85-x}Te_{15}In_x$.

Our calculated values of E_{MN} for $Se_{100-x}Te_x$ ($10 \leq x \leq 30$) alloy are between 67 and 75 meV. These are higher than those obtained by Mehta and Kumar [61]. This may be due to two different ways of estimating E_{MN}, one using the crystallisation rate and the other using the DC conduction rate equation.

Arora and Kumar [63] prepared $Se_{100-x}Te_x$ ($5 \leq x \leq 25$), $Se_{80-x}Te_{20}In_x$ ($0 \leq x \leq 25$), $Se_{100-x}Ge_x$ ($10 \leq x \leq 40$) and $Se_{68}Ge_{22}In_{10}$ glassy alloys using HQ method and studied the temperature dependence of DC conductivity. These authors estimated $E_{MN} = 69$ meV and $\sigma_{00} = 1.97 \times 10^{-2}\Omega^{-1}cm^{-1}$ for $Se_{100-x}Te_x$ ($5 \leq x \leq 25$) alloys. These results fairly agree with our calculated values of E_{MN} (67–75 meV) and σ_{00} = (0.24 to 2.08 $\Omega^{-1}cm^{-1}$) for $Se_{100-x}Te_x$ ($10 \leq x \leq 30$) alloys. A closer agreement for σ_{00} may be obtained for magnitude parameter $\alpha = 10^{-1}$, given in eq. (20).

Arora and Kumar [63] did not observe MN rule in the Ge-based alloys $Se_{100-x}Ge_x$ ($10 \leq x \leq 40$) and $Se_{68}Ge_{22}In_{10}$. However, Kumar *et al* [56] estimated $E_{MN} = 40.67$ meV and $\sigma_{00} = 3.78 \times 10^{-6}\Omega^{-1}cm^{-1}$ for $Se_{85-x}Te_{15}Ge_x$ ($x = 2, 4, 10$ and 15) alloys with their measurements for temperature dependence σ_{DC}. Our calculated values of E_{MN} for these alloys are 52 to 59 meV and σ_{00} are 1.45×10^{-2} to $4.60 \times 10^{-2}\Omega^{-1}cm^{-1}$. Thus, the calculated values of E_{MN} reasonably agree with the estimates of Kumar *et al* [56]. However, σ_{00} is larger by orders of magnitude and this suggests $\alpha = 10^{-4}$ for closer agreement.

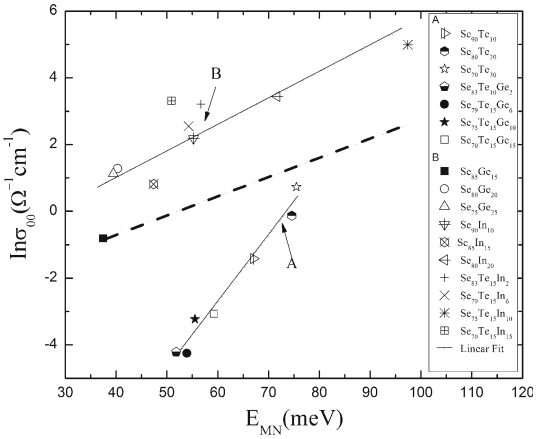

Figure 3. $\ln\sigma_{00}$ vs. E_{MN} for Se-based chalcogenides. The dashed line represents the overall linear relation $\ln\sigma_{00} = p_1 - q_1 E_{\mathrm{MN}}$, with $(p_1, q_1) = (-2.95, -0.057)$. The solid lines represent the linear relation with $(p_1, q_1) = (-14.64, -0.198)$ for group A materials and $(p_1, q_1) = (-2.124, -0.078)$ for group B materials.

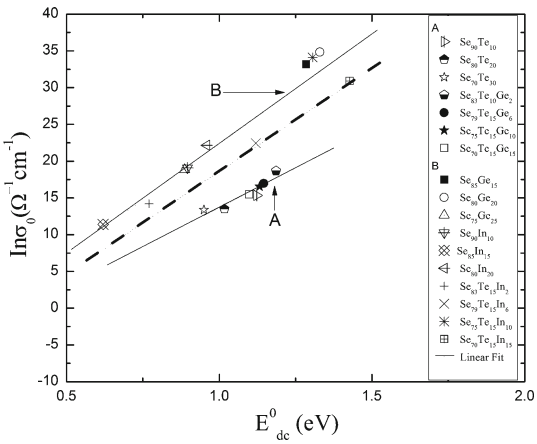

Figure 4. $\ln\sigma_0$ vs. E^0_{DC} for Se-based chalcogenides. The dashed line represents the overall linear relation $\ln\sigma_0 = p_2 - q_2 E^0_{\mathrm{DC}}$, with $(p_2, q_2) = (-9.41, -28.01)$. The solid lines represent the linear relation with $(p_2, q_2) = (-7.95, -21.64)$ for group A materials and $(p_2, q_2) = (-7.98, -30.27)$ for group B materials.

Arora and Kumar [63] also estimated $E_{\mathrm{MN}} = 68$ meV and $\sigma_{00} = 0.55 \times 10^{-2}\,\Omega^{-1}\,\mathrm{cm}^{-1}$ for $Se_{80-x}Te_{20}In_x$ $(0 \le x \le 20)$. However, with similar measurements, Kumar *et al* [56] estimated $E_{\mathrm{MN}} = 17.04$ meV and $\sigma_{00} = 1.678 \times 10^{-9}\,\Omega^{-1}\,\mathrm{cm}^{-1}$ for $Se_{85-x}Te_{15}In_x$ $(x = 2, 6, 15)$. Our calculated values of E_{MN}, 51 to 57 meV, agree with the estimates of Arora and Kumar [63] but higher than those of Kumar *et al* [56]. Similarly, our calculated σ_{00} between 12.88 and 27.67 $\Omega^{-1}\,\mathrm{cm}^{-1}$ agrees with that of Arora and Kumar [63] for $\alpha = 10^{-2}$. The results for the configuration $Se_{75}Te_{15}In_{10}$ are exceptionally higher.

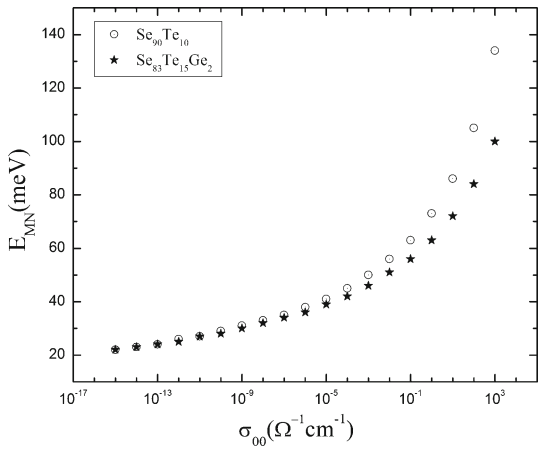

Figure 5. The variation of E_{MN} vs. σ_{00} $(\Omega^{-1}\,\mathrm{cm}^{-1})$ for $Se_{90}Te_{10}$ and $Se_{83}Te_{15}Ge_2$.

Our calculated values of σ_{00} for Se-based binary and ternary chalcogenides in the range of 10^{-2} $\Omega^{-1}\,\mathrm{cm}^{-1}$ to 10^{2} $\Omega^{-1}\,\mathrm{cm}^{-1}$ are higher by orders of magnitude than those found by Shimakawa and Abdel Wahab for As-based chalcogenides [12] and more close to those suggested by Emin *et al* [16]. The calculated values of E_{MN} agree with the experimental estimates and these are of the order of acoustic and optical phonon energies. Therefore, it is very likely that DC conduction in these Se-based chalcogenides may be due to acoustic and optical phonon-assisted polaron hopping and thermal compensation of DC conduction barrier height is significant.

Acknowledgements

The authors are thankful to Prof. G S S Saini, Ms Sameeksha Sharma and Ms Swati Khatta for their kind help. The financial support of DST with Grant No. SR/S2/CMP-28/2012 SERB is also acknowledged.

References

[1] C Hilseem, *Prog. Semicond.* **9**, 135 (1965)
[2] T J Coutts and N M Pearsall, *Appl. Phys. Lett.* **44**, 134 (1984)
[3] D L Staebler and C R Wronski, *J. Appl. Phys.* **51**, 3262 (1980)
[4] B Rosenberg, B B Bhowmik, H C Harder and E Postow, *J. Chem. Phys.* **49**, 4108 (1968)
[5] D P Almond, G K Duncan and A R West, *J. Non-Cryst. Solids* **74**, 285 (1985)
[6] J C Wang and Y F Chen, *Appl. Phys. Lett.* **73**, 948 (1998)
[7] W Meyer and H Neldel, *Z. Tech. Phys. (Leipzig)* **12**, 588 (1937)

[8] W B Jackson, *Phys. Rev. B* **38**, 3595 (1988)
[9] J C Dyre, *J. Phys. C* **19**, 5655 (1986)
[10] R S Crandall, *Phys. Rev. B* **43**, 4057 (1991)
[11] Y F Chen and S F Huang, *Phys. Rev. B* **44**, 13775 (1991)
[12] K Shimakawa and F Abdel-Wahab, *Appl. Phys. Lett.* **70**, 652 (1997)
[13] A Yelon and B Movaghar, *Phys. Rev. Lett.* **65**, 618 (1990)
[14] A Yelon and B Movaghar, *Appl. Phys. Lett.* **71**, 3549 (1997)
[15] N F Mott and E A Davis, *Electronic processes in non-crystalline materials* (Cladaron, Oxford, 1979) p. 428
[16] D Emin, C H Seager and R K Quinn, *Phys. Rev. Lett.* **28**, 813 (1972)
[17] S R Elliot, *Phil. Mag.* **36**, 1291 (1977)
[18] F Abdel-Wahab, *Phil. Mag. B* **82**, 1327 (2002)
[19] N Mehta, A S Mann and A Kumar, *Chalcogenide Lett.* **4**, 139 (2007)
[20] F Abdel-Wahab, A A Montaser and A Yelon, *Monatsh Chem.* **144**, 83 (2013)
[21] S Prakash, K Kaur, N Goyal and S K Tripathi, *Pramana – J. Phys.* **76**, 629 (2011)
[22] R Murti, S K Tripathi, N Goyal and S Prakash, *AIP Adv.* **06**, 035010 (2016)
[23] S Summerfield and P N Butcher, *J. Phys.* **15**, 7003 (1982)
[24] M H A Pramanik, P N Butcher and I D Cox, *Phil. Mag. B* **47**, 437 (1983)
[25] G E Pike and C H Seager, *Phys. Rev. B* **10**, 1421(1974)
[26] C Kittel, *Introduction to solid state physics*, 7th edition (John Wiley & Sons Pvt. Ltd., Singapore, 2001)
[27] S R Elliot, *Adv. Phys.* **36**, 135 (1987)
[28] S Mahadevan and A Giridhar, *J. Mater. Sci.* **29**, 3837 (1994)
[29] V Sharma, A Thakur, N Goyal, G S S Saini and S K Tripathi, *J. Optoelectron. Adv. Mater.* **7**, 2103 (2005)
[30] Z H Khan, M Zulfequar, A Kumar and M Hussain, *J. Phys. Condens. Matter* **80**, 19 (2002)
[31] M Lasocka, *Mater. Sci. Eng.* **23**, 173 (1976)
[32] R N Singh and Issam Ali, *Int. J. Appl. Phys. Math.* **3**, 275 (2013)
[33] A Comberg, S Ewert and H Wuhl, *Z. Phys. B* **25**, (1976)
[34] W Desorbo, *J. Chem. Phys.* **21**, 1144 (1953)
[35] N X Sun and K Lu, *Phys. Rev. B* **54**, 6058 (1996)
[36] A Zolanvari, N Goyal and S K Tripathi, *Pramana – J. Phys.* **63**, 617 (2004)
[37] Craig Russell, *Photodarkening of germanium–selenium glasses induced by below-bandgap light*, Ph.D. Thesis (University of Florida, USA, 2000)
[38] J Shirafuji, G I Kim and Y Inuishi, *Jpn J. Appl. Phys.* **16**, 67 (1977)
[39] H Oheda, *Jpn J. Appl. Phys.* **18**, 1973 (1979)
[40] J Sharma and S Kumar, *Pramana – J. Phys.* **86**, 1107 (2016)
[41] T Derrey, J M Saiter, J P Larmagnac and C Vautier, *Mater. Lett.* **3**, 308 (1985)
[42] R S Tiwari, N Mehta, R K Shukla and A Kumar, *J. Optoelectron. Adv. Mater.* **8**, 1211 (2006)
[43] H Y Lee, S H Park, J Y Chun and H B Chung, *J. Appl. Phys.* **83**, 5381 (1998)
[44] N Mehta, D Kumar, S Kumar and A Kumar, *Chalcogenide Lett.* **2**, 103 (2005)
[45] K Singh, N S Saxena, O N Srivastava, D Patidar and T P Sharma, *Chalcogenide Lett.* **3**, 33 (2006)
[46] R M Mehra, P C Mathur, A K Kathuria and Radhey Shyam, *Phys. Rev. B* **18**, 5620 (1978)
[47] Y Calventus, S Surinach and M D Baro, *J. Mater. Res.* **12**, 1069 (1997).
[48] N Mehta, R K Shukla and A Kumar, *Chalcogenide Lett.* **1**, 131 (2004)
[49] S Srivastava, M Zulfequar and A Kumar, *J. Ovonic Res.* **4**, 1 (2008)
[50] A Mandoza-Galvan, E Garcia-Garcia, Y V Vorobiev and J Gonzalez-Hernandez, *Microelectron. Eng.* **51–52**, 677 (2000)
[51] A Kumar, M Lal, K Sharma, S K Tripathi and N Goyal, *Indian J. Pure Appl. Phys.* **51**, 251 (2013)
[52] A Kumar, M Lal, K Sharma, P S Gill and N Goyal, *Chalcogenide Lett.* **11**, 249 (2014)
[53] B S Patial, N Thakur and S K Tripathi, *J. Therm. Anal. Calorim.* **106**, 845 (2011)
[54] A Sharma and P B Barman, *J. Therm. Anal. Calorim.* **96**, 413 (2009)
[55] R Ganesan, K N Madhusoodanan, A Srinivasan, K S Sangunni and E S R Gopal, *Phys. Status Solidi B* **212**, 223 (1999)
[56] A Kumar, M Lal, K Sharma, S K Tripathi and N Goyal, *Chalcogenide Lett.* **9**, 275 (2012)
[57] A Kumar, M Lal, K Sharma and N Goyal, *J. Non-Oxide Glass* **5**, 47 (2013)
[58] S K Tripathi, B S Patial and N Thakur, *J. Therm. Anal. Calorim.* **107**, 31 (2012)
[59] B S Patial, N Thakur and S K Tripathi, *J. Nano Electron. Phys.* **5**, 02017 (2013)
[60] A Miller and E Abrahams, *Phys. Rev.* **120**, 745 (1960)
[61] N Mehta and A Kumar, *J. Mater. Sci.* **42**, 490 (2007)
[62] C M Muiva, T S Sathiaraj, J M Mwabora and K Maabong, *Ceram. Int. A* **41**, 2348 (2015)
[63] R Arora and A Kumar, *Phys. Status Soldi A* **125**, 273 (1991)